CNRS
Centre National de la Recherche Scientifique

INFN
Instituto Nazionale di Fisica Nucleare

Measurements of Advanced Virgo OMC cavities finesse

Marine DUCROT, R. Bonnand, R. Gouaty, F. Marion,
A. Masserot, B. Mours, L. Rolland, M. Was

VIR-0458A-14

October 6, 2014

VIRGO * A joint CNRS-INFN Project
Project office: Traversa H di via Macerata - I-56021 S. Stefano a Macerata, Cascina (PI)
Secretariat: Telephone (39) 50 752 521 – Fax (39) 50 752 550 – e-mail virgo@pisa.infn.it

Contents

Introduction

The goal of the output mode cleaner (OMC) is to improve the interferometer contrast. The OMC parameters have been chosen to filter Higher Order Modes (HOM), see Appendix A, and radio frequency side bands for DC detection.

The Advanced Virgo OMC is a monolithic cavity with a bow-tie geometry. The finesse is determined by the reflectivity of each surface whereas the Radius of Curvature (RoC) is linked to the OMC spherical surface, see Appendix B. Specifications are $F = 142.5$ and $\rho = (1700 \pm 8)$ mm, see [6] and [9]. The finesse specification results from a tradeoff between minimizing the coupling of thermo refractive noise [6] and filtering out the 6 MHz side band (residual 6 MHz power in transmission of the OMC should stay below $80\,\mu$W).

This report summarizes the work on AdVirgo OMC cavities characterization, focusing on one parameter: the finesse F. It presents methods to determine this parameter and gives the results of these measurements.

We performed tests on four OMC substrates, OMC#8, OMC#6, OMC#7 and OMC#5[1].

Since cavities #5, #7 and especially #8 suffer from astigmatism, most of the tests have been made on cavity #6. But results are also given for cavities #5, #7 and to some extend for cavity #8.

[1]The number associated to OMC corresponds to the cavity polishing serial number and not to the cavity coating order

I Test bench and operations

A test bench has been implemented to measure the cavities finesse. The laser power is stabilized with a control loop, see figure 1. Two OMC supports have been placed on the bench with one of them in a vacuum chamber to be close to Advanced Virgo conditions.

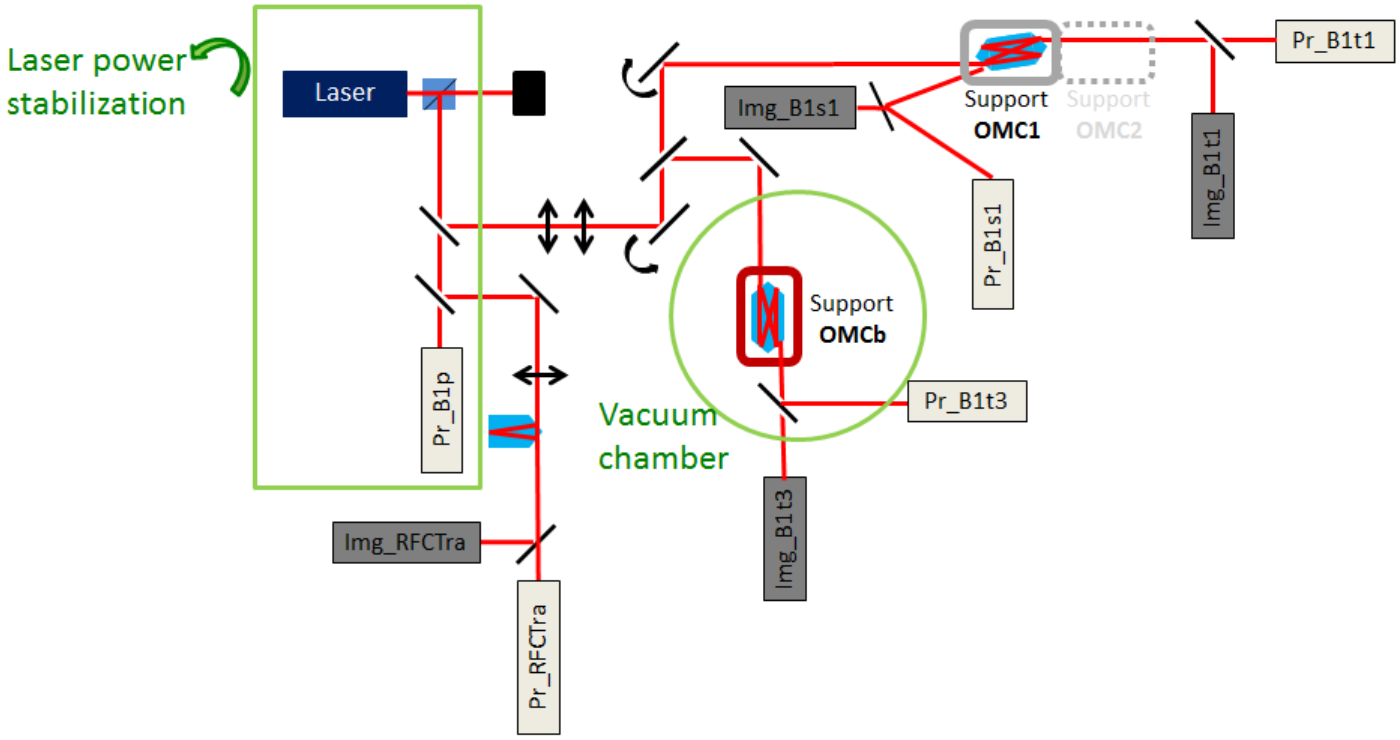

Figure 1: Scheme of the OMC test bench. The Pr and Img suffixes denote respectively photodiodes and CCD cameras.

The bench optical layout is shown in figure 1. The laser used is a Mephisto Nd-YAG with a $\lambda = 1064$ nm wavelength. The bench design is such that the beam waist is adapted to the cavity waist [3]. Several cameras and photodiodes are used to monitor the beams transmitted and reflected by each cavity. We use the cameras during the alignment of the beam onto the cavities to observe the transmitted high order modes (HOM). Pr_B1p is a pick off of the beam coming from the laser. Pr_ B1s1 measures the beam power reflected by the OMC1 and Pr_ B1t1 and Pr_ B1t3 measure the beams transmitted respectively by the OMC1 and OMCb. In this study, the OMC#6, #5 and #7 are on the OMC1 support, unless otherwise stated.

The OMC power transmission is defined as:

$$P_{DC} = \frac{P_{max}}{1 + \left(\frac{2F}{\pi}\right)^2 \sin^2\left(\frac{2\pi L_{opt}}{\lambda} - N \arccos\left(\sqrt{1 - \frac{2L_{geo}}{\rho}}\right)\right)} \tag{1}$$

Where we denoted in red the cavity parameters. $L_{geo} = 62.0$ mm is the geometric length (see Appendix B), $L_{opt} = 2nL_{geo}$ the optical length corresponding to an half a round trip of beam in the

cavity, $n = 1.44963$ the optical index, ρ the Radius of Curvature (RoC), F the finesse and N the mode order.

In the following, two methods are presented to scan the cavity resonance. We acted on two ways:

-Change of laser frequency ν (the laser scan method, see section I.2)

$$P_{DC} = \frac{P_{max}}{1 + \left(\frac{2F}{\pi}\right)^2 \sin^2\left(\frac{2\pi L_{opt}\nu}{c} - N \arccos\left(\sqrt{1 - \frac{2L_{geo}}{\rho}}\right)\right)} \tag{2}$$

-Change of cavity temperature (the temperature scan method, see section I.3), the cavity optical index changes with the cavity temperature, which in turns changes the optical length through $L_{opt} = 2nL_{geo}$. The cavity length changes slightly with temperature too. But the change of the cavity length L_{geo} with the temperature is negligible compared to optical index, see [2].

$$P_{DC} = \frac{P_{max}}{1 + \left(\frac{2F}{\pi}\right)^2 \sin^2\left(\frac{2\pi L_{opt}\nu}{c} - N \arccos\left(\sqrt{1 - \frac{2L_{geo}}{\rho}}\right)\right)} \tag{3}$$

We emphasize in green the parameter changed by each actuation method.

I.1 Controls on the bench

I.1.1 Laser power stabilization

Several control loops were used in the test set-up. Indeed to calculate the finesse value some parameters need to be stabilized: the laser power and the cavity temperature for a laser scan (see section I.2). The laser power was controlled, see figure 2, using the Pr_B1p photodiode, see figure 1.

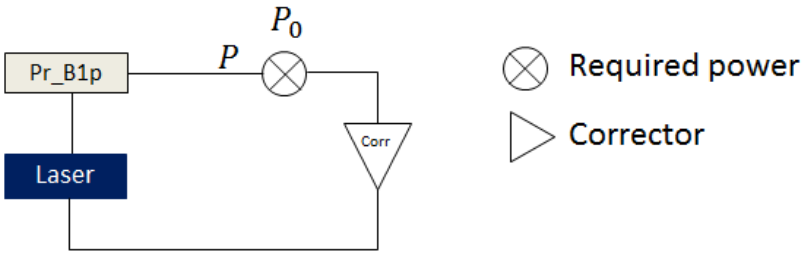

Figure 2: Control scheme of OMC power stabilization.

For a required power P_0, the error signal $P - P_0$ is used to determine the correction signal. This signal is applied with a Digital Analogue Converter (DAC) to the input of the laser control electronics unit, labelled "Current Laser Diode" [7]. This input controls the current of the diodes used to pump the laser crystal and thus the power delivered by the laser. With this control loop, the relative power fluctuation is: $\frac{\Delta P}{P} < 10^{-3}$ with ΔP the fluctuation $(P_{max} - P_{min})$ of the power P during five minutes, Figure 4.

I.1.2 Cavity temperature stabilization

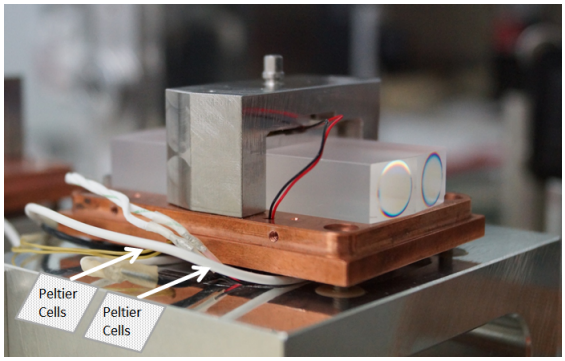

Figure 3: Peltier cells position on OMC support

A temperature probe is inserted in the copper support of the OMC measuring its temperature T. A couple of Peltier cells is located just underneath this copper support (see figure 3) to control the OMC temperature. For a required temperature T_0, the error signal $T - T_0$ is used to compute the correction signal, which is applied with a DAC to the Peltier cell driver board.

With this setup, the maximum fluctuations of the (in loop) temperature of the OMC base is ± 0.5 mDeg/10min (see for instance the bottom left plot of figure 4).

I.2 Laser scan

A laser scan is a triangular shape of the laser frequency over time, see upper right plot of figure 4. In order to act on the laser frequency a voltage is applied to the input of the laser control electronics unit which drives the temperature of the monolithic laser crystal. We can choose the amplitude, offset voltage and frequency of the scan.

In parallel, the OMC is stabilized in temperature with Peltier cells, explained in section I.1.2.

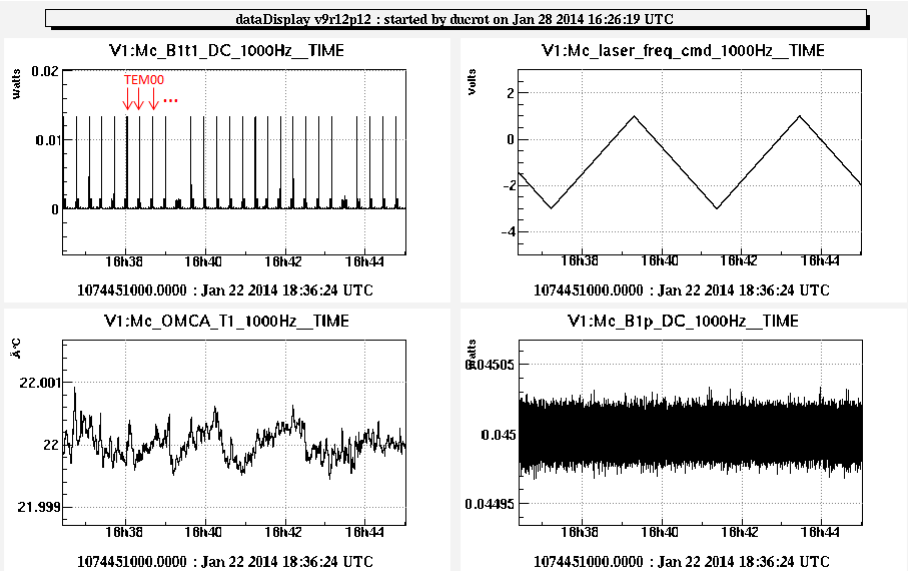

Figure 4: Laser scan. **Top**: On the left: power transmission of OMC over time. On the right: the voltage applied to the laser over time. Amplitude, offset and rate chosen here are respectively 4 V, -3 V and 0.004 Hz. **Bottom**: On the left: OMC stabilized temperature over time. On the right: the laser stabilized power over time.

The upper left plot of figure 4 shows the variation of power transmitted by the OMC over time during the scan. Each peak observed with Pr_B1t1 is an Airy peak corresponding to a TEM00 mode, see Appendix A. The distance between two TEM00 is the Free Spectral Range (FSR). The FSR for a laser scan is defined such as:

$$\Delta\nu = \frac{c}{2L_{opt}} \tag{4}$$

with $\Delta\nu$ the frequency variation, c the light celerity and L_{opt} the cavity optical length.

I.3 Temperature scan

A temperature variation changes the optical index and therefore the optical length, L_{opt}, used in formula (3). A temperature scan is a variation of the OMC temperature, controlled by Peltier cells, over time. We use again a triangular shaped signal for the requested temperature.

An FSR for a temperature scan is defined as:

$$\Delta L_{opt} = \frac{\lambda}{2} \tag{5}$$

with ΔL_{opt} the optical length variation corresponding to the temperature variation, $\lambda = 1064$ nm the wavelength.

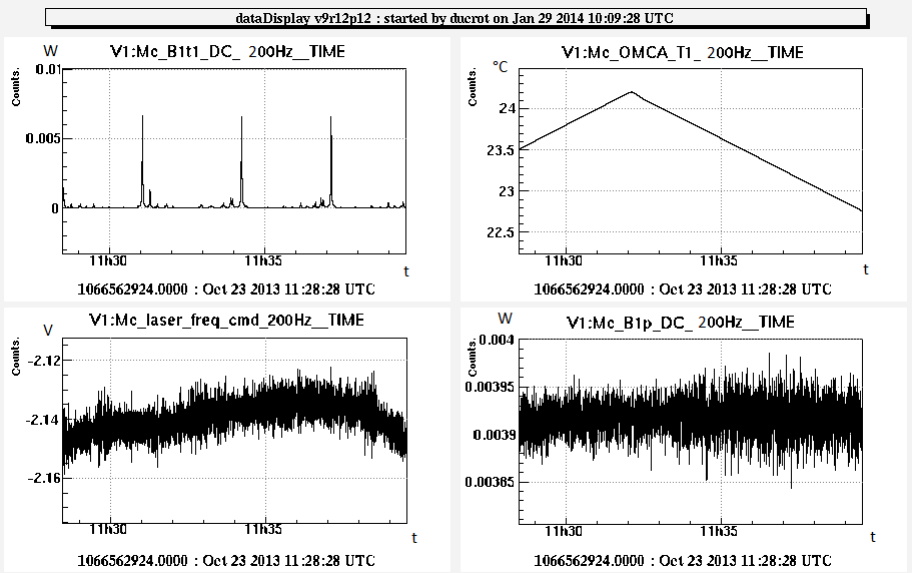

Figure 5: Temperature scan. **Top**: On the left: power transmission of OMC over the time. On the right: the OMC temperature change over the time. **Bottom**: On the left: frequency stabilization over the time. On the right: the laser power over time.

This plot informs us on the OMC behaviour as a function of temperature. For a temperature scan the distance between two peaks corresponds to a temperature variation of ≈ 0.55 °C. That highlights the importance of the OMC temperature stabilization for laser scan, see section I.2.

II Finesse from surface parameters

II.1 LMA measurements

The finesse definition is:

$$F = \frac{\pi\sqrt{r_1 r_2 r_3 r_4}}{1 - r_1 r_2 r_3 r_4} \tag{6}$$

where r_1, r_2, r_3, r_4 are reflectivities of each cavity surfaces [1] and figure 29 in Annexe B.

The finesse requested value was 142.5 [6]. LMA has measured, on test samples (i.e. not on the OMC themselves), the transmission and scattering losses values. Each batch of OMC has been coated with a test sample.

Transmission values found by the LMA on the test sample of batch 1 and 2 are in table 1.
The reflectivities can be computed using:

$$r_n = \sqrt{1 - T_n}\,, \tag{7}$$

where T_n is the transmission of surface n.
Moreover the scattering losses S were measured, see table 1.
Including losses the reflectivity is computed as:

$$r_n = \sqrt{1 - T_n - S_n} \tag{8}$$

with S_n, the scattering of surface n. Hence the expected finesse $F_{transmissionLMA}$ is reported in table 2.

Test samples		T	S
sample test of batch 1 (OMC#6 and #8)	entry surface	1.94%	5 ppm
	2^{rd} surface	2 ppm	50 ppm
	3^{rd} surface	2 ppm	28 ppm
	exit surface	2.18%	40 ppm
sample test of batch 2 (OMC#5 and #7)	entry surface	2.14%	22 & 20 ppm
	2^{rd} surface	4 ppm	40 & 11 ppm
	3^{rd} surface	4 ppm	8 & 9 ppm
	exit surface	2.10%	35 & 50 ppm

Table 1: Transmission T, scattering losses S. These measurements were made with an incidence angle of 6° on the surfaces in the air. Normally the angle should be 8.7° but this difference doesn't impact significantly the results.

	OMC#6 and #8	*OMC#7 and #5*
$F_{transmission\,LMA}$ *on test sample*	**150.5**	**146.3**

Table 2: Finesse taking into account scattering losses.

The impact of scattered losses on the finesse is order of 0.3% for the batch 1 and 0.2% for the batch 2. Thus the scattering losses have a negligible impact on the finesse values.

II.2 LAPP measurements

The LMA measurements have been done on test samples which are located in different positions in the coating machine. We decided to measure the power transmitted by substrate #6, #5 and #7 with the beam misaligned.

For the substrate #5 and #7 we performed two measurements based on two different alignment configurations in order to cross check our results. These two alignment configurations are denoted as "misalignment #1" and "misalignment #2" as shown in, figure 6 and 7.

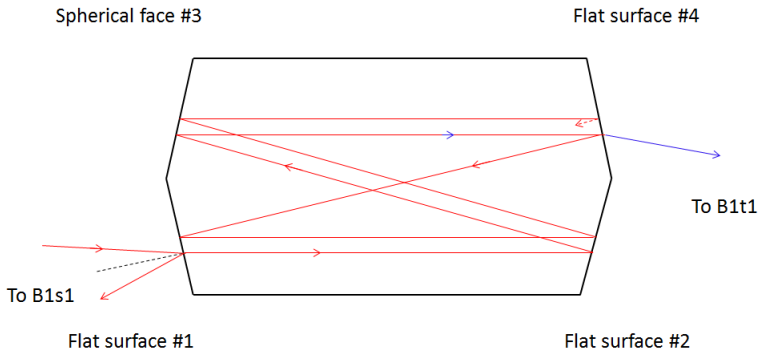

Figure 6: Misalignment of beam in the cavity. misalignment 1: OMC with a misaligned beam and separated round trips.

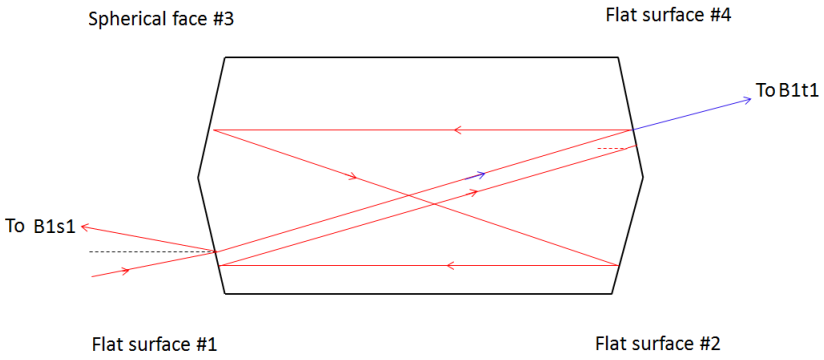

Figure 7: Misalignment of beam in the cavity. misalignment 2: the beam passes directly through the flat surfaces #1 and surface #4.

First we measure the input power, P_{input}. Indeed most of the input power is reflected by the entry surface. Then we measure the power transmitted through the OMC after a first (incomplete) round trip $P_{transmitted}$.

We measure the offset too (P_{offset}) and subtract it from previous measurements.

We obtained the transmissions average of surface #1 and #4 as we can neglige the transmission from surface #2 and #3 (table 1) :

$$T = \sqrt{\frac{P_{input}}{P_{transmitted} - P_{offset}}} \tag{9}$$

These results, especially for cavities #7 and #5, are lower than the value measured by LMA, see table 3. Given the difficulties of measurements, we chose to take as systematic errors, the largest deviation of a batch of measurements. We measured the finesse of OMC#6 only with the first method. The error of this measurement was not evaluated but is expected to be larger than the one of the other measurements.

OMC	#6	#7	#5
$F_{misaligment\,1}$	142.±?	125.0 ± 5.0	117.5 ± 5.0
$F_{misaligment\,2}$	–	125.0 ± 5.0	125.6 ± 5.0

Table 3: Finesse values by reflectivities of OMC#6, OMC#7, and #5 with two different misalignments and their systematic errors.

Furthermore the cavity internal losses measured at LAPP are approximatively equal to 1% for the OMC#6, see [10]. These losses are expected to be dominated by diffusion losses, which have been measured at LMA to be of the order of 1%. The agreement of these two values supports the hypothesis that the losses do not have a significant impact on the finesse.

OMC	#6	#5	#7
$Losses$	$< 1\%$	1.76%	1.4%

Table 4: Cavities losses of OMC#6, #7 and #5.

We also measured the losses for cavities OMC#7 and #5, see table 4. As for OMC#6, these values are closed to the values derived from the LMA measured scattering on the test samples, and confirm that as for the cavity #6, the losses of cavities #7 and #5 do not impact the finesse values.

III Measuring finesse from cavities scans

In this section, we present the finesse values obtained from the scan of a full spectral range (FSR, i.e. the distance between two TEM00), either by changing the laser frequency ('laser scans') or by changing the cavity optical length ('temperature scans'), as sketched in figure 8.

III.1 Finesse calculation method

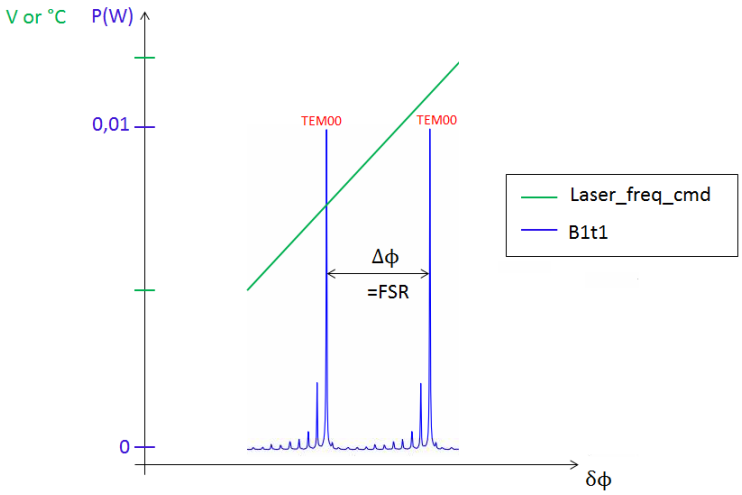

Figure 8: Beams power transmitted by OMC over time (in blue), laser frequency or laser temperature change linearly over $\delta\Phi$ (in green). With $\delta\Phi$ the electromagnetic wave phase.

Equation 1 can be reformulated as:

$$P_{DC}(\delta\Phi) = \frac{P_{max}}{1 + \left(\frac{2F}{\pi}\right)^2 \sin^2\left(\delta\Phi\right)}\,, \tag{10}$$

with $\delta\Phi$ the electromagnetic wave phase, see figure 9.

For any power we can write:

$$P_{DC}(\frac{d\Phi}{2}) = pP_{max} \tag{11}$$

with p a percentage, $d\Phi$ the width at the power pP_{max}, see figure 9.

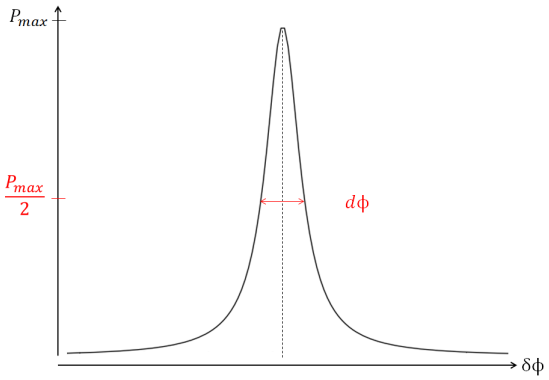

Figure 9: TEM00 Airy's peak. Here $d\Phi$ is the full width at half-maximum of an Airy peak ($P_{DC} = 0.5P_{max}$) associated with the TEM00 resonance.

Finally, injecting formula (11) in formula (10) we obtain:

$$\boxed{F = \sqrt{\frac{1}{p} - 1}\frac{\Delta\Phi}{2\sin(\frac{d\Phi}{2})}} \tag{12}$$

with $\Delta\Phi = \pi$ a FSR, the distance between two TEM00 (see figure 8).

Remark: Here the scans are done over time. So we can convert the electromagnetic wave phase into the equivalent time evolution.

i.e:

$$F = \sqrt{\frac{1}{p} - 1}\frac{\Delta\Phi}{2\sin(\frac{dt\times\pi}{\Delta t\times 2})} \tag{13}$$

with dt the width at half-maximum of an Airy peak expressed in seconds and Δt the FSR in seconds.

III.2 Details on finesse measurement

When we compute the finesse, we want also to estimate systematic errors of the measurement caused by external effects (incident power, speed of the scan, ...). For this reason we distinguish the applied voltage slope (up or down) and the side of the peak (left or right), see figure 10.

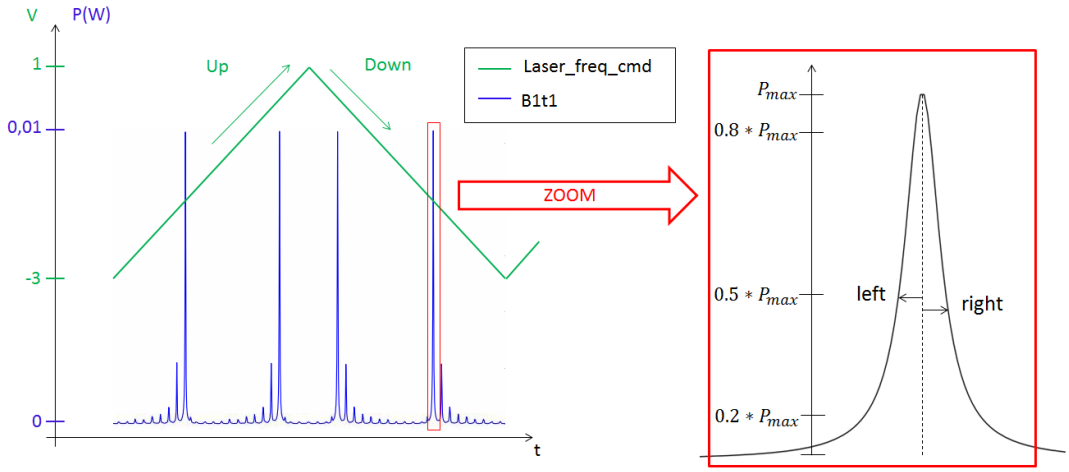

Figure 10: Right and left width. Up going and down going slope.

In order to collect large statistics and reduce errors we use a program that measures the finesse from a long measurement.

The first step of the program is to process the data to record the short data segments which contains peaks, see figure 11:

-The program reads 2000 points of data. The sampling frequency is 1000 Hz.

-This chunk of 2000 points is divided in four parts, $\left[\frac{0}{4};\frac{4}{4}\right]$.

-The program processes the 1000 points of the central part (segment $\left[\frac{1}{4};\frac{3}{4}\right]$), searching for peaks exceeding a threshold of about 70% of the maximum observed during the full data taking. If a peak is found, this segment of 2000 data sample is recorded for detailed analysis as described later.

-The program moves to the next segment, sliding the data by 500 points.

This method allows to not miss any peak even if the reading stops in middle of the peak and avoids memory overloading.

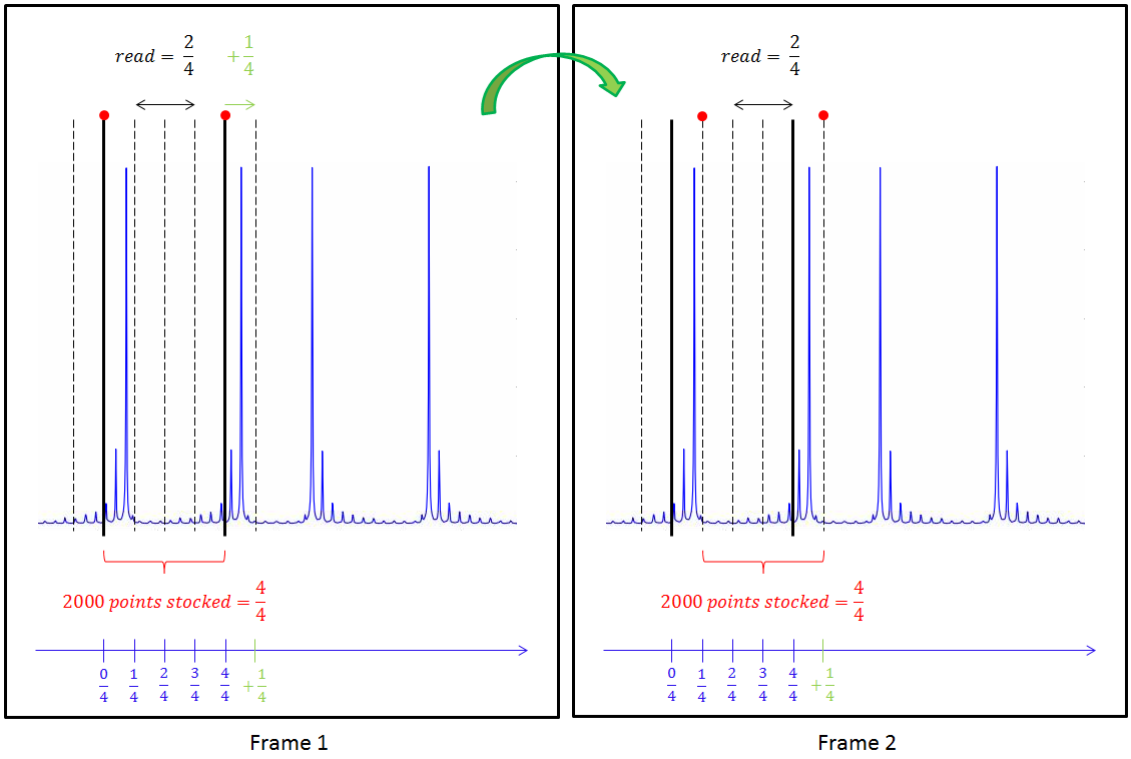

Figure 11: Representation of data processing

The second step of the program is to extract the peak parameters from the collected snip of data around the peak.

We have seen (in section III.1) that we can compute the finesse with different peak widths. We decided to use the peak width at $0.8P_{max}$, $0.5P_{max}$ and $0.2P_{max}$, see figure 10. Data are processed for one peak as following:

-We fit a parabola on the maximum point of the segment and the two adjacent points to find precisely its position, see figure 12.

-This fit is used to compute the maximum value, P_{max}, and consequently the heights (at $0.8P_{max}$, $0.5P_{max}$ and $0.2P_{max}$).

-For each peak height, a regression is done on three points at the left and the right of the peak, see figure 12. We obtain the widths at 0.8, 0.5 and 0.2 of the maximum power and we can distinguish right and left widths with the position of maximum.

-The direction of the scan (up or down) is recorded too.

Finally with these parameters we can compute the finesse value. To this purpose we compute the average widths of the two peaks of a FSR to obtain the width used in the finesse computation, see part III.1.

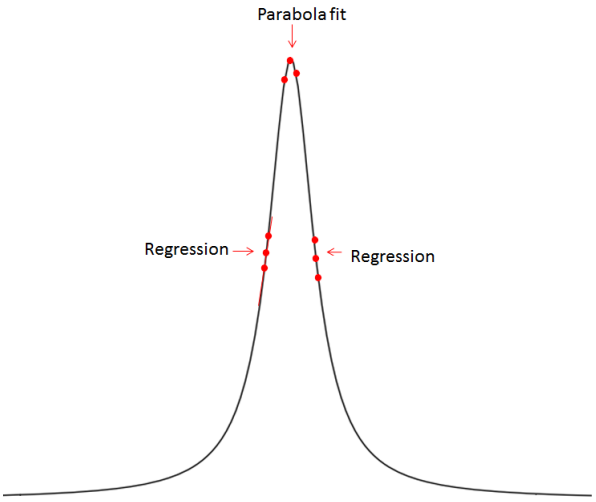

Figure 12: Representation of the parabolic fit near the peak maximum and regression at $0.5P_{max}$

IV Finesse from cavities laser scans

IV.1 Electronic artefact in finesse measurements

In order to characterize the OMC#6, we performed some laser scans with different parameters. We changed the speed, the laser power and other parameters.

On some of our first measurements, we noticed an asymmetry between "right" and "left" finesse[2]. The right finesse was always larger than the left finesse, regardless if the cavity length or laser frequency was increasing or decreasing. This asymmetry turned out to be due to an instrumental artefact: the analogue shaping filter of the photodiode was not properly compensated by the correcting digital filter, leading to a frequency dependant response of the overall reading chain of the transmitted beam. Therefore the time delay of the chain was not the same on the sides of the peak and on the top of the peak (due to the difference in slope i.e. frequency) introducing the left/right asymmetry. This effect was only present when the speed of the scan requires the use of data in the bad frequency band.

The first line of figure 13 shows the worst cases observed for this effect, while the bottom line shows the measurements made on the same cavity but with a correct electronic chain.

The electronic chain has been fixed at the end of the campaign of measurement, and we keep in this report only the results which were not affected by this effect.

[2]See part III.2

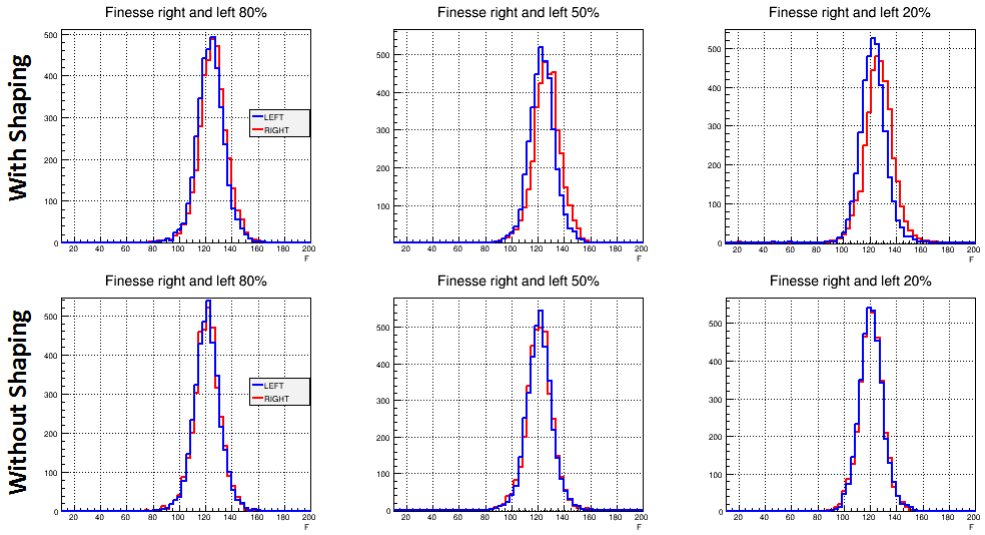

Figure 13: OMC#6. Scans with and without shaping filter made on 07/18/2014. Finesse values found with width at 80%, 50% and 20% of peak maximum power. In red the right width, in blue the left width.

IV.2 Effects of laser power on the finesse measurement

To check that no thermal effect was biasing the finesse measurement, we performed three sets of scans at 4, 8 and 12 mW.

IV.2.1 Measurement at one power 8 mW

Technical sheet of scan

$Date$	07/18/2014
OMC	#6
$B1p(mW)$	8
$Amplitude\ (V)$	4
$Offset(V)$	-2
$Frequency(Hz)$	0,002
$Peltiers$	$22°C$

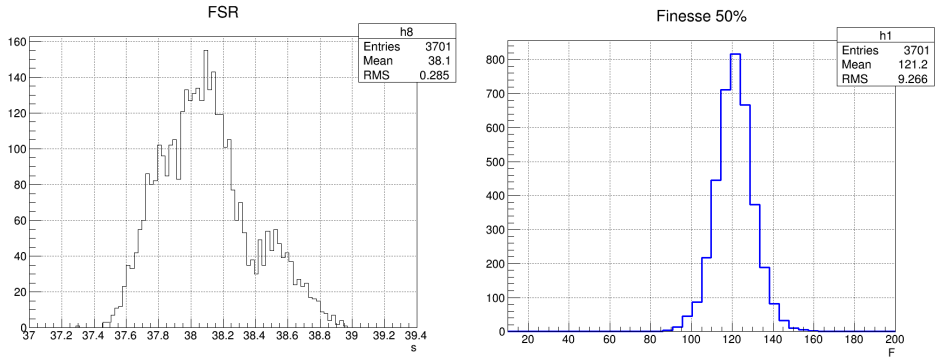

Figure 14: On the left, parameter of scan: amplitude, offset and frequency are the parameters of the triangular signal driving the laser frequency. The center plot is the histogram of all the measured FSR, the right one presents the distribution of the finesse values. For these parameters, a FSR is scanned in 38.1 seconds.

Figure 14 presents one of this scan. The RMS of the FSR histogram shows us that the FSR lengths are more stable than the finesse (0.7% for FSR versus 7% for finesse). Therefore, the fluctuations of the finesse are coming from the fluctuation of the peaks widths.

The histograms of the extracted finesse values are reported in the following figures.

When we change the direction of scan (up or down) we change the order of apparition of HOM, see I.2. A finesse left up corresponds to a finesse right down. That's why we have assembled finesse

left up and right down and finesse right up and left down, see figure 15. To search for systematic effect, we have gathered scan up and down and scan right and left. No systematic bias is observed.

Moreover we have distinguished on the figure 16 the finesses left and right at 80%, 50% and 20%.

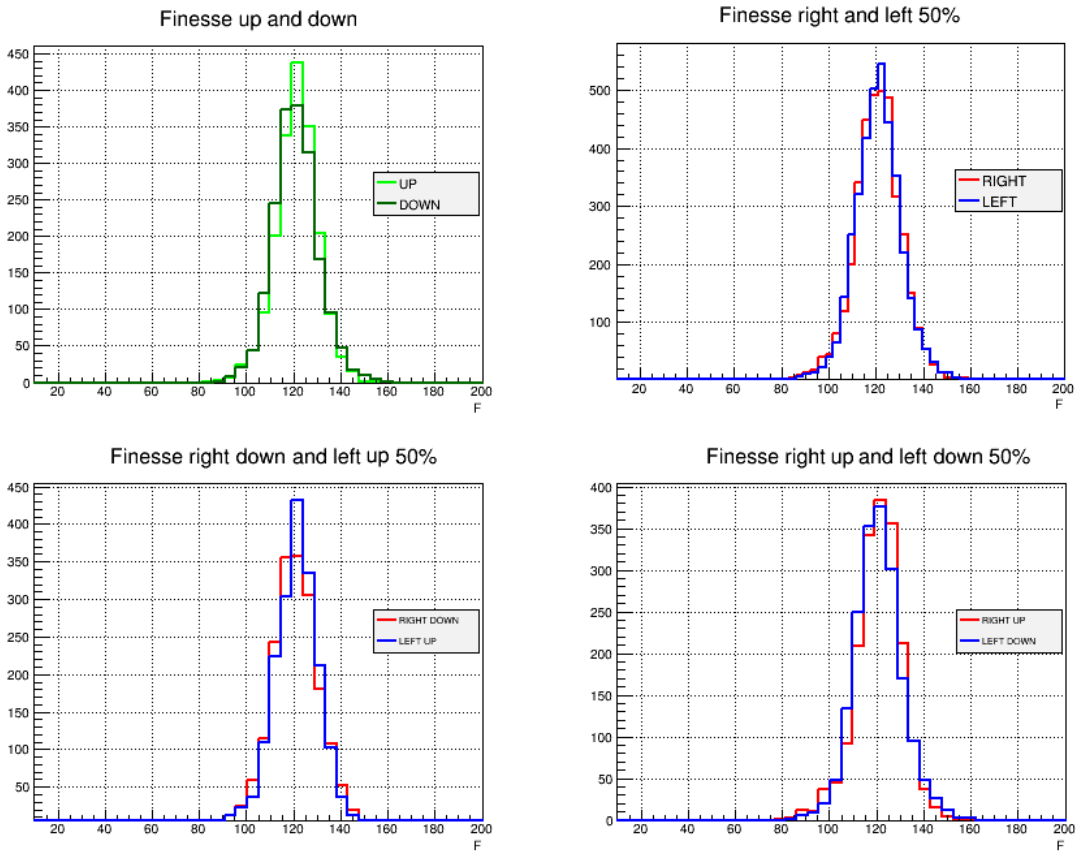

Figure 15: Finesse values with some distinct parameters (up, down, right, left etc...) defined in part III.2 at $P = 0.5P_{max}$. The mean values are reported in table 5.

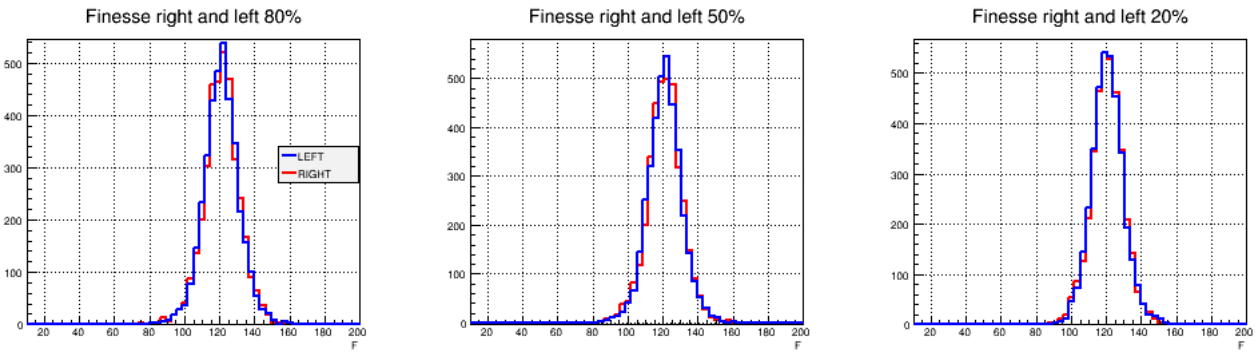

Figure 16: Finesse values found with width at 80%, 50% and 20% of peak maximum power. In red the right width, in blue the left width. The mean values are reported in table 5.

IV.2.2 Comparison of results at different power

Figures 17 and 18 present scans performed at 4 and 12 mW. Similarly to the scans performed for 8mW, the FSR lengths are more stable than the finesse at 4 and 12 mW.

Technical sheet of scan

$Date$	07/17/2014
OMC	#6
$B1p(mW)$	4
$Amplitude\ (V)$	4
$Offset(V)$	-2
$Frequency(Hz)$	0,002
$Peltiers$	$22°C$

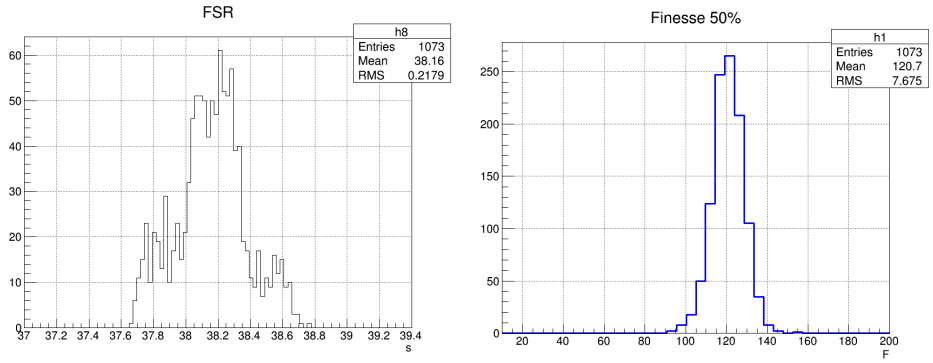

Figure 17: On the left, parameter of scan. Amplitude, Offset and frequency are the parameters of the triangular signal driving the laser frequency. The center plot is the histogram of the FSR, the right one is presents the finesse values. For these parameters, a FSR is performed in 38.2 seconds.

Technical sheet of scan

$Date$	07/24/2014
OMC	#6
$B1p(mW)$	12
$Amplitude\ (V)$	4
$Offset(V)$	1
$Frequency(Hz)$	0,002
$Peltiers$	$22°C$

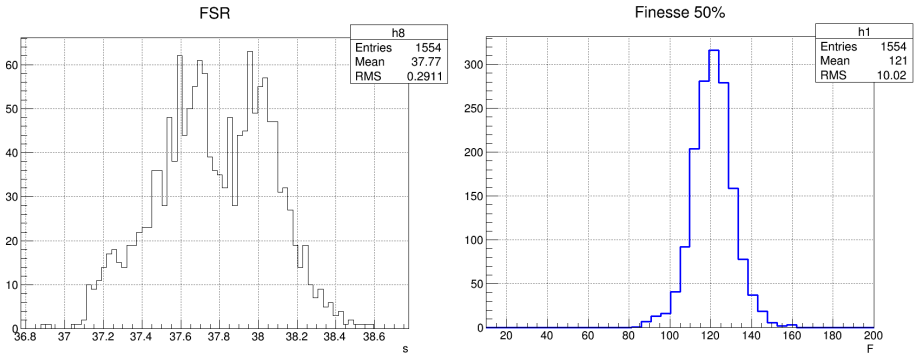

Figure 18: On the left, parameter of scan. Amplitude, Offset and frequency are the parameters of the triangular signal driving the laser frequency. The center plot is the histogram of the FSR, the right one is presents the finesse values. For these parameters, a FSR is performed in 37.8 seconds.

Table 5 summarizes the finesse and width values of OMC#6. Like for the finesse computed from the surface parameters measured at LAPP (see II.2), the finesse values from the laser scans are lower than expected. The average is 121.2. The spread of the measurements (using only the finesse from the full width) indicates a systematic error of about ± 1 on the finesse value.

If there were effects of thermal lensing we would expect to observe a difference between up and down scans. When the power of TEM00 is at maximum the OMC heats up. If we are on the up slope of the laser scan, this change of temperature impacts on the OMC optical index and have for effect to slow the scan (the peak part after resonance). It's the contrary for a down scan. None of these effects seem to be observed. Nevertheless we observe a difference between up and down but this difference is not always in the same direction ($F_{up} < F_{down}$ or $F_{up} > F_{down}$). Conclusion: there are not systematic effects from laser power stabilization.

$OMC\#6$	07/17/14		07/21/14		07/24/14	
$Laser\ power\ (mW)$	4		8		12	
$Amplitude\ (V)$	4		4		4	
$Frequency\ (Hz)$	0.002		0.002		0.002	
$Nbr\ FSR$	1073		1547		1554	
$F_{80\%}$	120.8 ± 0.2		121.1 ± 0.2		121.0 ± 0.2	
$F_{50\%}$	120.7 ± 0.2		121.5 ± 0.2		121.0 ± 0.2	
$F_{20\%}$	120.2 ± 0.2		120.6 ± 0.2		120.6 ± 0.2	
	$Left$	$Right$	$Left$	$Right$	$Left$	$Right$
$F_{80\%up}$	121.1	121.3	120.9	120.9	120.8	120.8
$F_{50\%up}$	121.2	121.0	120.9	120.8	120.7	120.6
$F_{20\%up}$	121.0	120.3	121.1	120.5	120.4	120.8
$F_{80\%down}$	120.7	120.4	121.3	121.5	121.5	121.3
$F_{50\%down}$	120.6	120.2	121.2	121.3	121.5	121.0
$F_{20\%down}$	120.0	120.0	120.6	121.1	121.6	120.3

Table 5: Finesse values versus laser power. Errors are only statistical.

IV.3 Scan speed influence on the finesse measurement

To further study systematic effects, we did some scans with different scan velocities. The results are reported in table 6.

The only observed trend is a slight increase of the finesse for the slowest scan. For these slowest scan, the dispersion of the measurements are larger, making this slight difference not very significant.

$OMC\#6$	07/26/14		07/18/14		07/23/14	
$Laser\ power\ (mW)$	8		8		8	
$Amplitude\ (V)$	4		4		4	
$Frequency\ (Hz)$	0.001		0.002		0.004	
$Nbr\ FSR$	2289		3701		4060	
$F_{80\%}$	123.3 ± 0.3		121.1 ± 0.2		120.5 ± 0.1	
$F_{50\%}$	122.6 ± 0.3		121.2 ± 0.2		121.3 ± 0.1	
$F_{20\%}$	121.6 ± 0.3		120.6 ± 0.2		120.6 ± 0.1	
	$Left$	$Right$	$Left$	$Right$	$Left$	$Right$
$F_{80\%up}$	122.0	122.8	121.2	121.1	120.0	120.6
$F_{50\%up}$	121.4	122.7	121.2	120.9	119.6	120.9
$F_{20\%up}$	121.1	122.6	121.1	120.7	119.1	121.8
$F_{80\%down}$	125.0	125.1	121.0	121.2	121.1	120.4
$F_{50\%down}$	124.1	124.3	120.9	121.0	121.4	120.0
$F_{20\%down}$	123.5	123.0	120.4	120.8	122.2	119.4

Table 6: Finesse values versus scan frequency. Errors are only statistical.

IV.4 Stabilization temperature influence on the finesse measurement

To determine the temperature stabilization influence on the computed finesse we have drawn the peak width (in time) versus the ΔT observed during a TEM00 peak Figure 19. The ΔT is in degree and corresponds to the range between the minimum and the maximum of the temperature recorded during the peak. The plots 19 shows that there is no correlation between the temperature fluctuation and the width at half height.

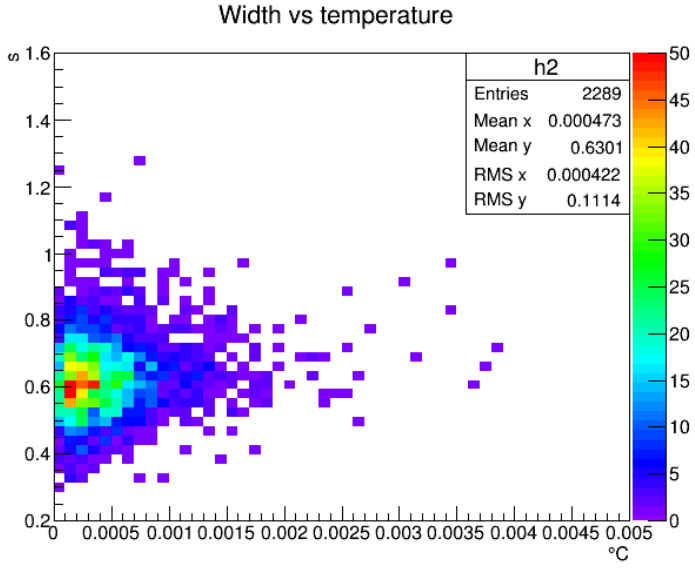

Figure 19: Width at 50% of peak maximum power versus delta temperature. 07/06/2014, $\nu = 0.001Hz$.

IV.5 DAC noise influence on the finesse measurement

In this part we search if we are limited by the noise of the DAC driving the laser frequency. Indeed the DAC sensitivity is different depending on the applied voltage. The low frequency DAC noise increases when the request voltage increases, see figure 20.

To see if we are limited by this noise, we have compared the widths of TEM00 at $0.2P_{max}$, $0.5P_{max}$ and $0.8P_{max}$ between $[-0.5V; 0.5V]$ and for a voltage outside this range (to 2 V) . The results are presented on the figure 21 and table 7. The widths and consequently the finesses don't seem to be limited by the DAC sensitivity. If that was the case the width values near $0V$ would be with a RMS lower than the other widths. It's not actually the case.

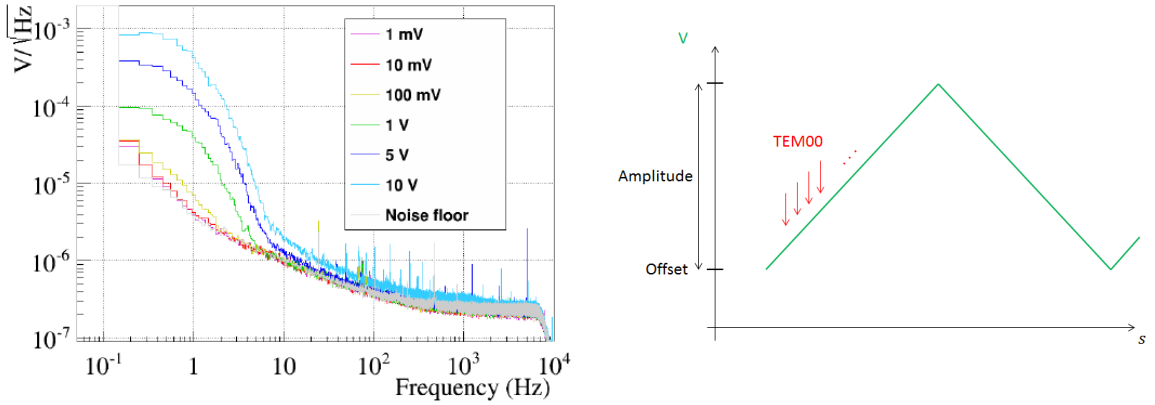

Figure 20: Left: DAC signal with DC inputs, see [8]. Right: In green ramp applied on laser to have a laser scan, in red the peaks that we can find along this ramp.

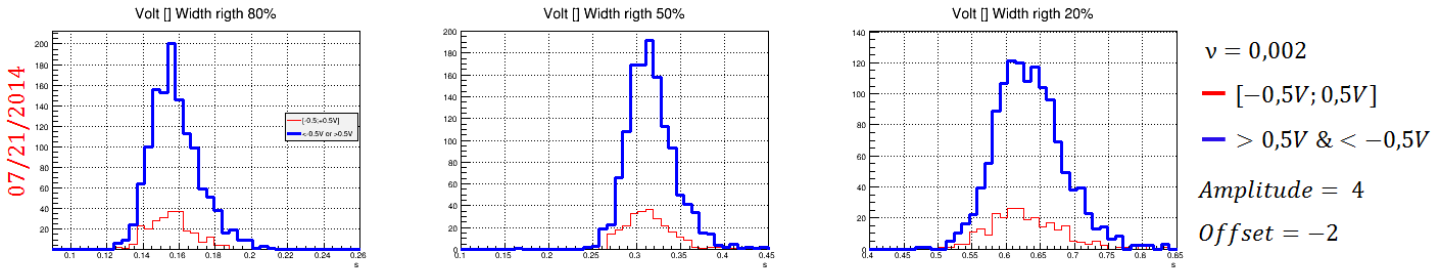

Figure 21: Widths at 20%, 50% and 80% of peak maximum power. In red the peak widths measured when the DAC absolute voltage is limited to a 0.5 V, in blue the other cases.

$07/21/2014\,\nu = 0.002Hz$	$Entries$	$Mean$	rms
$Width\,0.8P_{max}\,[-0.5V, 0.5V]$	258	0.156	0.014
$Width\,0.8P_{max}\,< -0.5V\ or\ > 0.5V$	1289	0.158	0.014
$Width\,0.5P_{max}\,[-0.5V, 0.5V]$	258	0.313	0.027
$Width\,0.5P_{max}\,< -0.5V\ or\ > 0.5V$	1289	0.3162	0.027
$Width\,0.2P_{max}\,[-0.5V, 0.5V]$	258	0.628	0.053
$Width\,0.2P_{max}\,< -0.5V\ or\ > 0.5V$	1289	0.634	0.049

Table 7: Width at 20%, 50% and 80% of peak maximum power.

IV.6 Effect of the sampling frequency on finesse measurement

Since some early data were collected at only 200 Hz instead of 1 kHz, we checked that the finesse computation wasn't affected by the data sampling rate. To check that, we resample offline a 1 KHz data set at 200 Hz and extract the finesse in this two set of data corresponding to the same measurement. The result is reported in table 8. No effect is observed.

$OMC\#6$	$07/21/14\,1000Hz$	$07/21/14\,200Hz$
$Laser\,power\,(mW)$	8	8
$Amplitude\,(V)$	4	4
$Frequency\,(Hz)$	0.002	0.002
$Nbr\,FSR$	1547	1547
$F_{80\%}$	121.1 ± 0.2	121.1 ± 0.2
$F_{50\%}$	121.5 ± 0.2	121.4 ± 0.2
$F_{20\%}$	120.6 ± 0.2	120.5 ± 0.2
F_{up}	121.3 ± 0.2	121.3 ± 0.2
F_{down}	121.6 ± 0.2	121.6 ± 0.2
F_{right}	121.1 ± 0.2	121.1 ± 0.2
F_{left}	121.0 ± 0.2	121.1 ± 0.2

Table 8: Right column, result for the 200 Hz resampled data set, left column results from the original data set at 1 kHz.

IV.7 OMC#6 average finesse from laser scans

We have six finesse values at $0.5P_{max}$ (see table 5 and 6) corresponding to scans with different parameters (different laser power and speed scans). The finesse average weighted by statistical errors is:

$$F_{average} = \left(\sum_i \frac{1}{\delta F_i^2} \right)^{-1} \sum_i \frac{F_i}{\delta F_i^2} \;=\; 121.3 \pm 0.1 \tag{14}$$

with δF_i the statistical errors and i the different measurements.

The given uncertainties are statistical errors. We have seen that different conditions led to slightly shifted values of finesse. The average of the biggest and smallest observed shifts is used to estimate the systematic uncertainties. Therefore, the OMC#6 finesse value is, including systematic uncertainties:

$$\boxed{F_{average} = 121.3 \pm 2.9} \tag{15}$$

IV.8 Finesse values of OMC#7, #5 and #8

The OMC#7 and #5 are from the same batch of coating. The results of the measurement are reported in Table 9. We observe the same finesse within 1% for each OMC. These finesses values extracted by scans confirm the finesse values found by transmission measurements done at LAPP (section II).

	08/01/2014	08/11/2014	08/28/2014
OMC	#7	#5	#8
$Laser\,power\,(mW)$	8	8	8
$Amplitude\,(V)$	4	4	4
$Frequency\,(Hz)$	0.004	0.004	0.002
$Temperature\,(°C)$	25	22	22
$Nbr\,FSR$	9668	2016	1080
$F_{80\%}$	124.7 ± 0.1	123.9 ± 0.1	126.6 ± 0.3
$F_{50\%}$	124.6 ± 0.1	124.2 ± 0.1	126.4 ± 0.3
$F_{20\%}$	124.1 ± 0.1	123.8 ± 0.1	125.8 ± 0.3
F_{up}	124.5 ± 0.1	124.4 ± 0.1	127.0 ± 0.3
F_{down}	124.7 ± 0.1	124.0 ± 0.1	125.9 ± 0.3
F_{right}	124.6 ± 0.1	124.1 ± 0.1	126.6 ± 0.3
F_{left}	124.6 ± 0.1	123.8 ± 0.1	126.4 ± 0.3

Table 9: Finesse values for OMC#7, OMC#5 and OMC#8.

V Finesse from cavities temperature scans

To investigate the systematic errors from frequency scan, we proceeded at a different type of measurement: the temperature scans.

This measurement is a little more complex since the temperature control for a temperature scan is not linear during the whole ramp period. When the scan direction changes from up to down (or from down to up) Peltier cells don't provide a linear response. The FSR lengths are modified. That's why

we have taken the FSR which are only on the ramp middle part, between $22°C$ and $24°C$. Despite that, we observe three sets of values on the FSR histogram figure 23. These three sets correspond to three types of FSR duration. If the finesse value is not impacted by the different FSR sets, the non linear response of Peltier cells leave a little tail on the finesse histogram that comes from the peaks widths.

Figure 22 shows the main signals during a typical temperature scan. The histograms of the extracted finesse values are reported in the following figures 23 and 24. The small tail at low finesse value might slightly bias the mean value toward low finesse values. The finesses values are given in table 10.

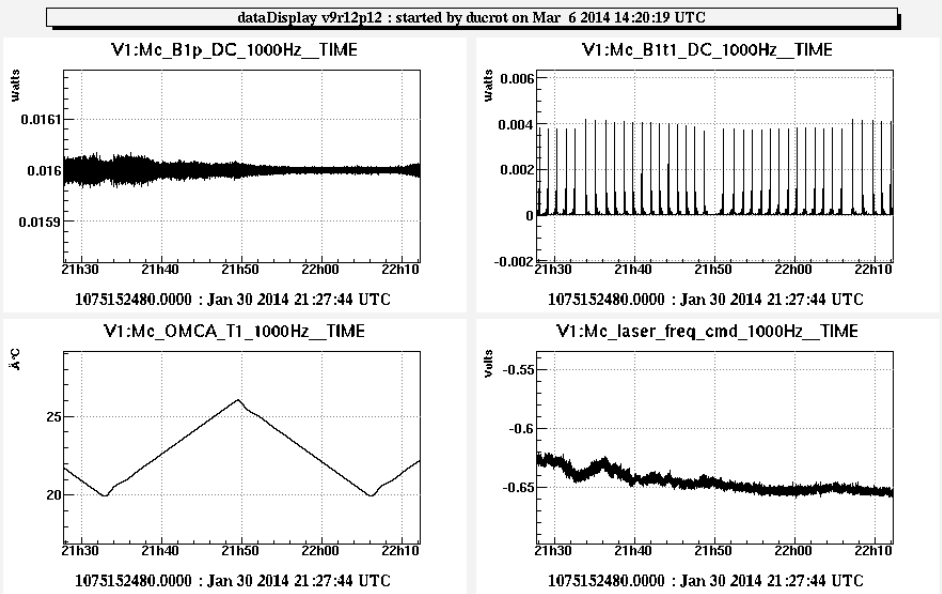

Figure 22: Temperature scan of 01/30/2014. The upper left plot shows the OMC incident power during part of a scan. The lower left plot is showing the temperature of the cavity support when the Peltier cells are driven by a triangular signal. The upper right plot shows the transmitted beam power, while the cavity is going through many FSR. The lower right plot shows the signal of the laser frequency command, which uses an external cavity for frequency stabilization.

Technical sheet of scan

Date	08/08/2014
OMC	#6
B1p(mW)	8
Amplitude (°*C*)	6
Offset(°*C*)	20
Frequency(*Hz*)	0,001

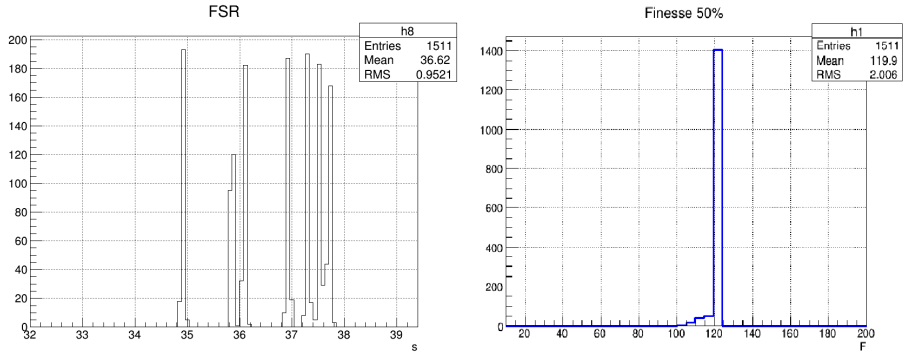

Figure 23: On the left: parameters of the scan. On the middle: histogram of FSR values measured for temperature between $22°C$ and $24°C$. On the right: the finesse histogram.

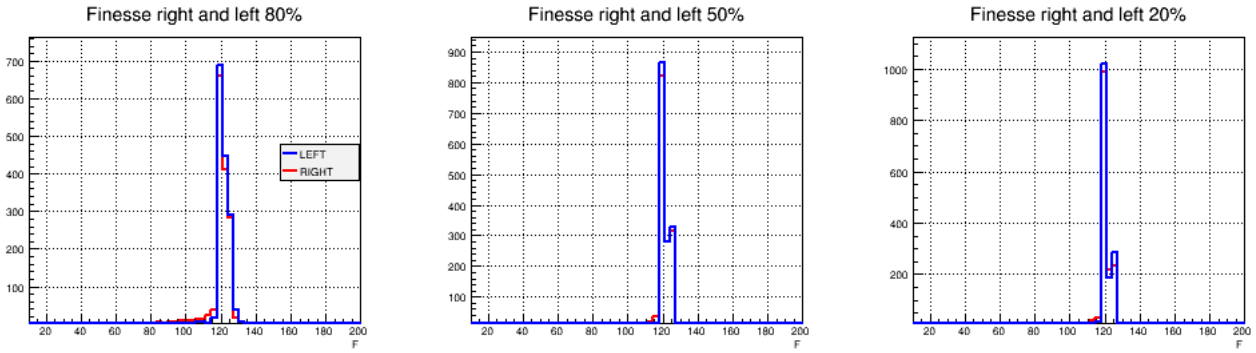

Figure 24: Finesse distributions, estimated with the peak width at 3 different heights. See table 10 for the mean values.

$OMC\#6$	08/08/14	
$Laser\,power\,(mW)$	8	
$Amplitude\,(°C)$	6	
$Frequency\,(Hz)$	0.001	
$Nbr\,FSR$	1511	
$F_{80\%}$	120.8 ± 0.1	
$F_{50\%}$	119.9 ± 0.1	
$F_{20\%}$	120.9 ± 0.1	
	$Left$	$Right$
$F_{80\%\,up}$	121.1 ± 0.1	120.1 ± 0.1
$F_{50\%\,up}$	121.0 ± 0.1	120.6 ± 0.1
$F_{20\%\,up}$	120.6 ± 0.1	120.7 ± 0.1
$F_{80\%\,down}$	121.8 ± 0.1	120.7 ± 0.1
$F_{50\%\,down}$	121.9 ± 0.1	121.3 ± 0.1
$F_{20\%\,down}$	121.8 ± 0.1	120.8 ± 0.1

Table 10: Finesse obtained with a temperature scan.

The finesse values obtained from temperature scans (see table 10) are the same as the finesse values from laser scans (see equation (15)): around 121 for the cavity #6.

We observe that the finesse distribution is larger for frequency scans (see figure 16) than for temperature scans (see figure 24). One possible hypothesis is that the combination of commands of power and frequency sent to the laser are interacting, yielding a noisy laser beam. To check this hypothesis we did some laser scans without the power stabilization control loop but this did not change the RMS of the finesse distribution. Therefore another plausible hypothesis is that the laser frequency control is creating a noisy beam affecting the beam widths estimations.

VI Finesse values for polarizations S and P

The finesse values presented up to now have been measured with an S polarized beam, thanks to a polariser cube placed at the laser exit.

However, a PZT actuator is placed on top of the cavity to modulate the cavity optical length and to produce an error signal for the cavity control. This strength applied on top of the cavity creates birefringence and therefore two polarization states resonating at two different frequencies in the cavity.

To measure the P polarized cavity finesse we placed a wave plate before the OMC entry with a proportion of 41% of polarization S (59 % of polarization P). Then we put a polariser cube on the transmitted beam to select the P polarized component and extract the corresponding finesse. Figure 25 shows the corresponding plots.

We repeat this measurement, changing the output polariser cube to extract the S polarized finesse. Figure 26 shows the corresponding plots. The S polarization result is in agreement with the values reported in the previous sections since, in normal measurement conditions, the P component is small and produce resonances peaks at different positions than from the S component.

The overall results are presented in table 11. The difference between the two polarizations is not very important since the beams are hitting the reflective surface with an incident angle not too far from normal incidence, and therefore the reflection coefficients for a P polarized beam are not very different than the ones for the normal S polarized beam.

Technical sheet of scan

$Date$	08/11/2014
OMC	#6 pol-P
$B1p(mW)$	8
$Amplitude\ (V)$	4
$Offset(V)$	-2
$Frequency(Hz)$	0,004
$Peltiers$	$22°C$

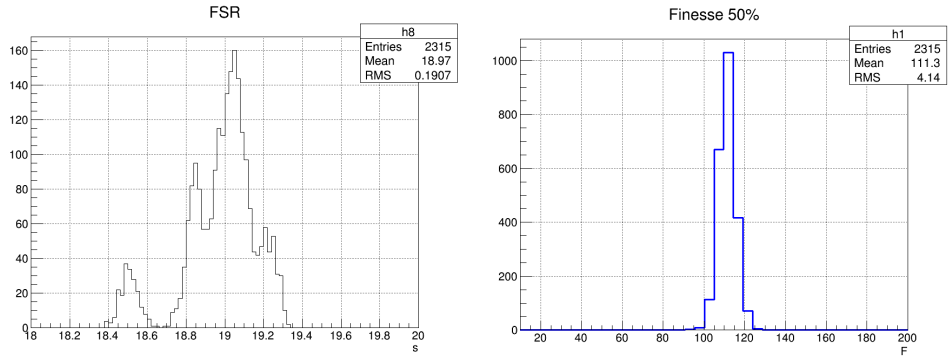

Figure 25: Summary of the measurements with a P polarized beam.

Technical sheet of scan

$Date$	08/12/2014
OMC	#6 pol-S
$B1p(mW)$	8
$Amplitude\ (V)$	4
$Offset(V)$	-2
$Frequency(Hz)$	0,004
$Peltiers$	$22°C$

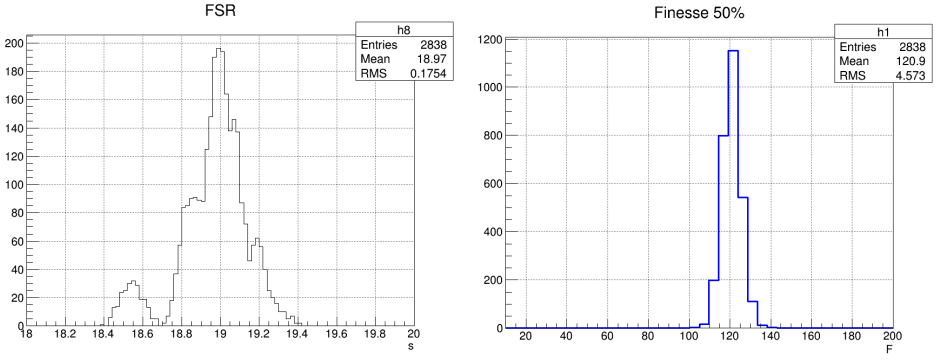

Figure 26: Summary of the measurements with an S polarized beam.

$OMC\#6\,pol-S$	08/12/2014
$Laser\,power\,(mW)$	8
$Amplitude\,(V)$	4
$Frequency\,(Hz)$	0.004
$Temperature\,(°C)$	22
$Nbr\,FSR$	2838
$F_{80\%}$	120.2 ± 0.1
$F_{50\%}$	120.9 ± 0.1
$F_{20\%}$	120.3 ± 0.1

$OMC\#6\,pol-P$	08/11/2014
$Laser\,power\,(mW)$	8
$Amplitude\,(V)$	4
$Frequency\,(Hz)$	0.004
$Temperature\,(°C)$	22
$Nbr\,FSR$	2016
$F_{80\%}$	110.9 ± 0.1
$F_{50\%}$	111.3 ± 0.1
$F_{20\%}$	110.0 ± 0.1

Table 11: Finesse values for OMC#6 with polarisation S and P.

$$\boxed{F_{pol-S} = 121.3 \pm 2.9} \tag{16}$$

$$\boxed{F_{pol-P} = 110.7 \pm 2.9} \tag{17}$$

Conclusion

This report describes the measurements and results obtained for the finesse of the AdV OMC cavities. The specification for the finesse was 142.5.

The finesses derived from the LMA transmission measurements on two test samples placed near to cavities surface during the coating process are:

	test sample 1 ($OMC\#8$ *and* $OMC\#6$)	*test sample* 2 ($OMC\#7$ *and* $OMC\#5$)
F	150.5	146.3

The finesses derived from the LAPP transmission measurements of the cavities surfaces are:

OMC	#6	#7	#5
$F_{misaligment\,1}$	142.0±?	125.0 ± 5.0	117.5 ± 2.0
$F_{misaligment\,2}$	–	125.0 ± 5.0	125.6 ± 5.0

We did several finesse measurements using the laser frequency scan technique. Using the first OMC cavity we had, cavity #6, we investigated the systematic errors of the measurements, changing the incident power, the speed of the scan, looking at effect from sampling rate or DAC noise. We did also cavity optical length scans via temperature scans. All these measurements give consistent results, in agreement with the finesse value derived from the LAPP transmission measurements (except for cavity #6 for which the quality of LAPP transmission measurement is rather poor). These results are:

OMC	#6	#7	#5	#8
F	121.3 ± 2.9	124.6 ± 2.9	124.2 ± 2.9	126.4 ± 2.9

These finesses are lower than the ones extracted from the measurements of the cavity surfaces transmissions made at LMA on a test sample. It has also been checked that cavity losses are small and dominated by scattering losses. They are of the order of what was expected from the specifications and cannot explain the observed differences for finesse values. Nevertheless, it should be reminded that the LMA transmission measurements are not made on the surfaces of the cavities but on the test samples located next to the cavities, which might explain the differences.
A preliminary study of the impact of a finesse lower than specifications has been discussed during the two last Virgo weeks [4] [5].

References

[1] L. Derome, 1999, Le système de détection de l'expérience VIRGO dédiée à la recherche d'ondes gravitationnelles

[2] A. Dominjon, 1996, Recherche des ondes gravitationnelles avec l'interferomètre Virgo: étude et conception de l'ensemble de détection du signal

[3] M. Ducrot, 2013, Stage M2, Caractérisation de la cavité « mode cleaner » en sortie de l'interferomètre Advanced Virgo

[4] M. Ducrot, R. Bonnand, R. Gouaty, F. Marion, A. Masserot, B. Mours, L. Rolland, M. Was, Measurement of AdV OMC cavities finesse (Virgo meeting May 2014, Cascina), VIR-0260A-14

[5] M. Ducrot, R. Bonnand, R. Gouaty, F. Marion, A. Masserot, B. Mours, L. Rolland, M. Was, AdV OMC cavities measurements (Virgo meeting September 2014, Cascina), VIR-0419A-14

[6] R. Gouaty, R. Bonnand, F. Marion, B. Mours, L. Rolland, 2013, Advanced Virgo Output Mode Cleaner: Optimization of the cavity parameters to minimize the thermo-refractive noise, VIR-0016A-13

[7] Mephisto Product Line, User's Manual, InnoLight GmbH, Hannover, 30.10.2003

[8] N. Letendre, A. Masserot, B. Mours, E. Pacaud, S. Petit, L. Rolland, J. Tassan, 2014, Prototype of the DAC1955 mezzanine for AdV DAQ-Box

[9] The Virgo Collaboration, April 13, 2012, Advanced Virgo Technical Design Report p235 à 263

[10] R. Bonnand, A. Masserot, M. Was, R. Gouaty, M. Ducrot, L. Rolland, B. Mours, F. Marion, Advanced Virgo OMC test (LVC meeting March 2014, Nice), VIR-0093A-14

Appendix

A. Hermite-Gauss and Laguerre-Gauss modes

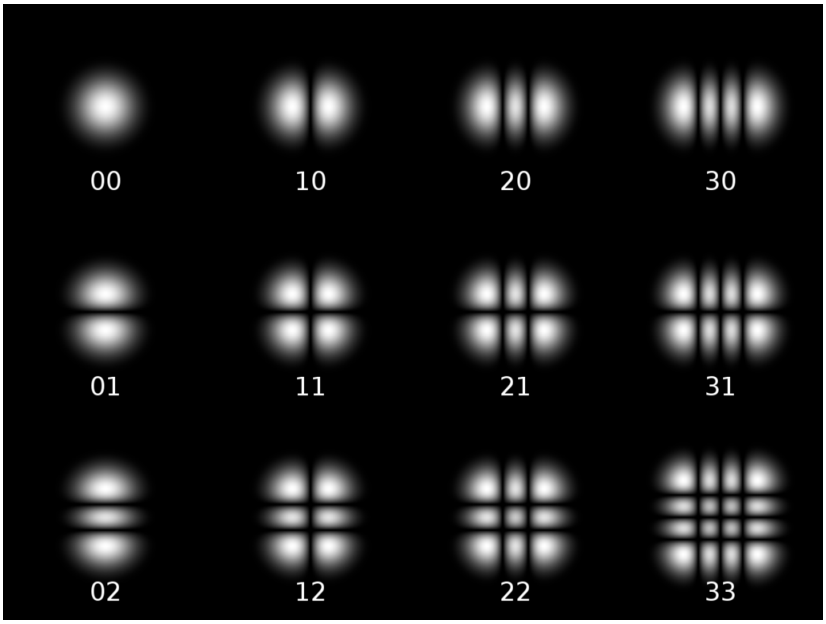

Figure 27: Hermite-Gauss modes

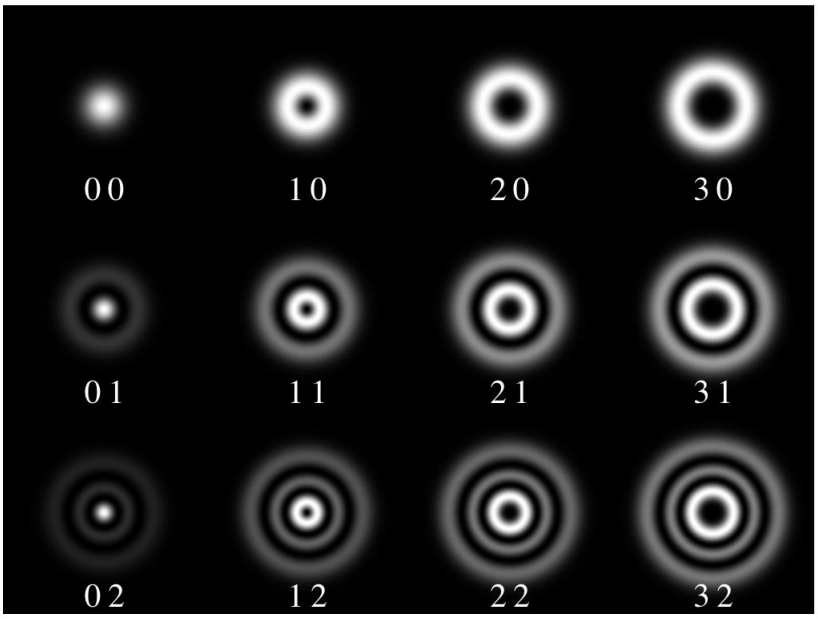

Figure 28: Laguerre-Gauss modes

B. AdVirgo OMC cavity geometry

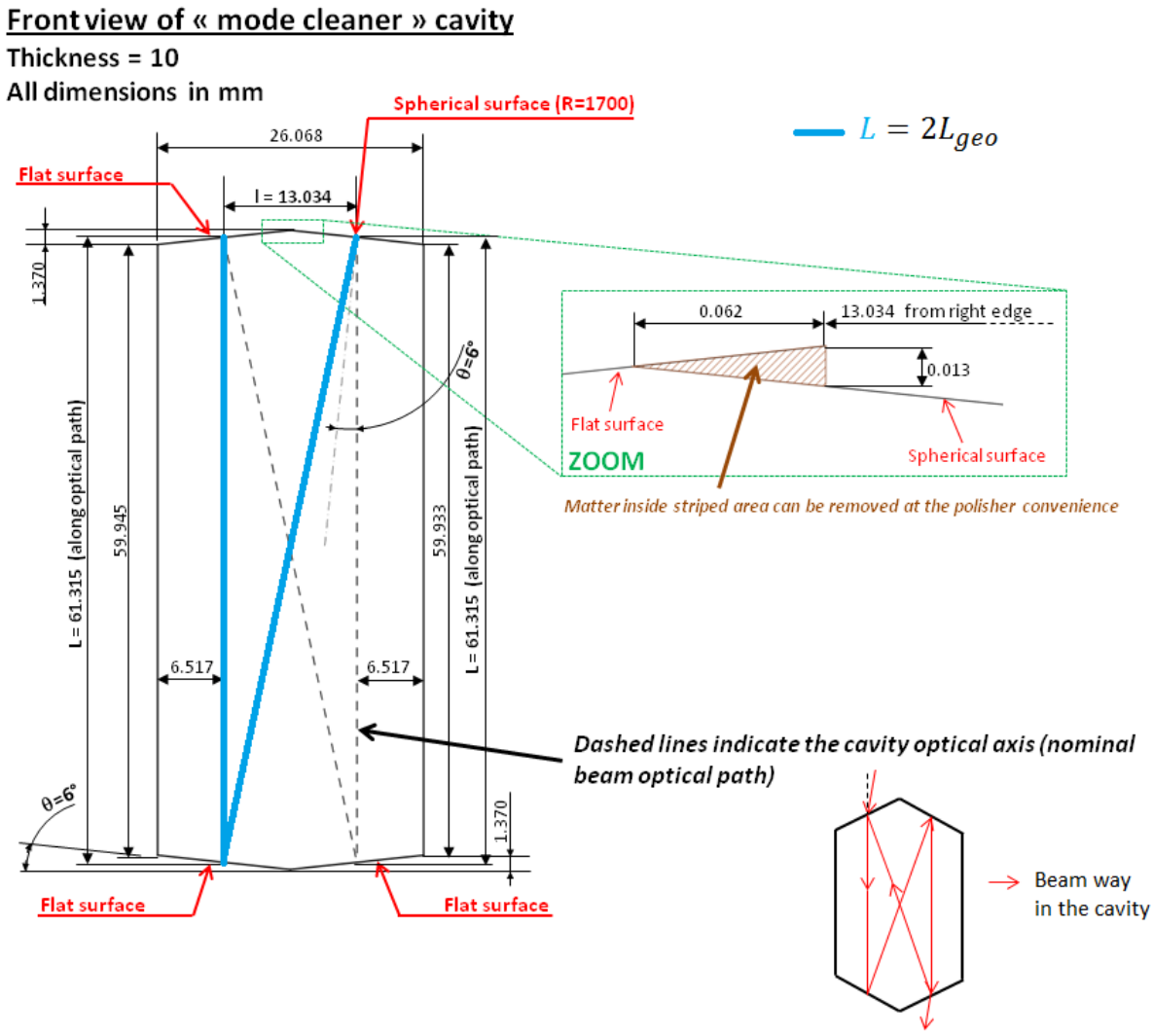

Cavity Length (as measured along the beam optical path between two opposite surfaces)	L = (61.315 ± 0.200) mm
Distance between the optical centers of two adjacent surfaces	l = (13.034 ± 0.100) mm
Inclination angle of each surface	θ = (6.00 ± 0.03) degrees
Radius of curvature of the spherical surface	R = (1700 ± 8) mm

Tab.1: Main geometrical parameters of the mode cleaner cavity with allowed manufacturing error bars.

Diameter of the clear aperture on each surface	8 mm
Surface flatness defects (over the clear aperture of 8 mm)	5 nm RMS, or λ/40 PtV (λ=1064 nm)
Micro-roughness (spatial frequencies above 1000m^{-1}) within the clear aperture	≤ 0.3 nm RMS
Scratch/Digs within the clear aperture	5/1x0.02 ; L1x0.003 Or best effort

Tab.2: Specifications for the polishing quality of the four mode cleaner reflective surfaces.

Figure 29: The OMC AdVirgo specifications